28. N. S. Morrissette, V. Bedian, P. Webster, D. S. Roos, *Exp. Parasitol.* **79**, 445 (1994).
29. Extracellular tachyzoites were fixed for 1 hour on ice in 4% PBS-buffered formaldehyde and then for 12 hours at 4°C in 8% PBS-buffered formaldehyde. The cell suspension was embedded in 10% gelatin, incubated for 2 hours at 4°C in PBS containing 2.3 M sucrose, and frozen in liquid nitrogen. Ultrathin sections of the frozen samples were freshly prepared before each hybridization experiment. Cryosections were transferred to grids and digested for 40 min at 37°C in 2× SSC containing 200 μg/ml of DNase-free RNase A. Cellular DNAs were denatured for 5 min at 70°C in 70% formamide (in 2× SSC), chilled on ice, transferred to 50% formamide (in 2× SSC), and incubated briefly at 25°C. Sections were hybridized for 12 hours at 37°C in a humidified chamber in 5 μl of hybridization mix containing 10 to 20 ng/μl of DNA probe (*26*), washed three times for 5 min at 25°C in 4× SSC, twice for 3 min at 37°C in 50% formamide (in 2× SSC), twice for 5 min at 25°C in 2× SSC, and kept in 4× SSC at 25°C before staining. Hybridized probe was detected with polyclonal sheep anti-digoxigenin, followed by a secondary rabbit antibody directed against sheep immunoglobulin G (Pierce), and Protein A conjugated to 10-nm particles of gold. Immunogold-labeled sections were blocked for 20 min at 25°C in 4× SSC containing 0.5% blocking reagent and were incubated with a monoclonal antibody against DNA, followed by a rabbit anti-mouse secondary antibody and protein A conjugated to 5-nm gold particles. To improve the contrast of membranous structures, we counterstained hybridized cryosections on ice for 10 min in 0.3% aqueous uranyl acetate plus 2% methylcellulose. Grids were air-dried on loops and examined with a Phillips EM400 microscope.
30. The antibody directed against DNA used in Fig. 2A probably recognizes both endogenous DNA and the digoxigenin-labeled probe. Similarly, the 5-nm gold–protein A conjugate used to visualize this antibody (by means of a secondary rabbit antibody) is potentially able to recognize any anti-digoxigenin that remained unblocked. Comparable staining with antibody against DNA was observed even in the absence of a DNA probe, however (Fig. 2C), or when control plasmid was used as a probe. Cryosections labeled with antibody to DNA before the application of anti-digoxigenin also showed co-localization of large and small gold particles. The apparent clustering of label in Fig. 2, A and B, may be an artifact of in situ hybridization conditions, because antibody directed against DNA labels the organelle uniformly (Fig. 2C).
31. Infected cultures were fixed for 45 min in freshly prepared 50 mM phosphate buffer (pH 6.3) containing 1% glutaraldehyde and 1% OsO_4, rinsed in distilled water, stained in 0.5% uranyl acetate overnight, dehydrated, and embedded in Epon. Ultrathin sections were picked up on uncoated grids, stained with uranyl acetate and lead citrate, and examined with a Phillips 200 electron microscope.
32. A total of 65 sequences, including nearly all available bacterial sequences and representative plastid sequences, were aligned using PILEUP [Genetics Computer Group, Madison, WI (1991)], with manual refinement on the basis of secondary structural information. Maximum likelihood analysis was performed with fastDNAml v1.0.6 [G. J. Olsen, H. Matsuda, R. Hagstrom, R. Overbeek, *CABIOS* **10**, 41 (1994)], compiled as parallel code running on an Intel Paragon 64-node partition. Three random addition sequences and global swapping were used, but it cannot be guaranteed that the tree found is the highest likelihood tree possible. Bootstrap data sets and consensus trees were generated using PHYLIP tools SEQBOOT and CONSENSE [J. Felsenstein, University of Washington, Seattle, WA (1993)]. Bootstrap replicates were analyzed with fastDNAml using a single random addition sequence and local branch swapping only. LogDet, parsimony, and constraint analyses were performed with PAUP*4.0d48 [D. L. Swofford; Smithsonian Institution, Washington, DC (1996)] using nucleotide data from the first and second codon positions, and bootstrapping was carried out using 100 replicates with random addition sequences (where appropriate). LogDet distances are not directly comparable to standard distances but yield additive distances under any Markov model when sites are evolving independently and at the same rate (*9*).
33. This work was supported by NIH grants AI-31808 (D.S.R.) and GM-52857 (L.G.T.), NSF grant DEB-93–18594 (J.D.P.), and the University of Pennsylvania Program in Computational Biology. P.W.D. was supported by a Medical Research Council studentship, and R.J.M.W. by the United Nations Development Program–World Bank–World Health Organization Special Programme for Research in Tropical Diseases. D.S.R. is a Burroughs Wellcome New Investigator in Molecular Parasitology and a Presidential Young Investigator of the NSF, with support from Merck Research Laboratories and the MacArthur Foundation. We wish to thank R. G. K. Donald for molecular clones derived from the *T. gondii* 35-kb element, L. Chicoine for assistance with cryosectioning, J. F. Dubremetz for suggesting that the apicomplexan plastid described herein be designated the apicoplast, and P. Kuhlman, F. Lutzoni, K. Pryer, and D. Williamson for helpful discussions.

16 September 1996; accepted 27 December 1996

TECHNICAL COMMENTS

Evidence for a Family of Archaeal ATPases

The analysis by Carol J. Bult *et al.* of the *Methanococcus jannaschii* genome included families of paralogous proteins that did not seem to have counterparts in the current sequence databases (*1*). The largest of such families consists of 13 chromosomal and three plasmid-encoded proteins, which were found to be highly similar to one another [figure 6 in (*1*)], but did not show statistically significant similarity to any proteins, thus escaping functional prediction. Our inspection of the alignment, however, indicates that two of the conserved sequence blocks correspond to well-characterized functional motifs: namely, the phosphate-binding P-loop and the Mg^{2+}-binding site that are conserved in a vast variety of ATPases and GTPases (Fig. 1 and *2–4*). Even though most commonly used methods for database search such as BLASTP (*5*) showed only marginally significant similarity to several ATPases, a new version of the BLASTP program that constructs local alignments with gaps (*6*) indicated a probability of matching by chance between 10^{-4} and 10^{-6} for some of the proteins in the new archaeal family and bacterial DnaA proteins; the conservation was particularly notable in the two ATPase motifs (Fig. 1). Thus, even though these 16 proteins comprise a novel family that is so far represented only in archaea, they appear to belong to a known broad class of proteins, and we predict that they possess ATPase activity.

Screening of the nonredundant protein sequence database at the National Center for Biotechnology Information (National Institutes of Health, Bethesda, MD), with a bipartite pattern representing the specific forms of the two ATPase motifs conserved in the *M. jannaschii* family—namely, hhhhGx_4-GK[TS]$x_n$hhhhD[DE] (h indicates a bulky hydrophobic residue), selected 271 proteins, all of which are either known to possess ATPase activity or are highly similar to ATPases. In addition to DnaA, this list includes a number of members of the so-called AAA ATPase family (*7*); the similarity between these proteins and DnaA has been noted before (*4*). Many of the AAA family proteins possess chaperone-like activity and, in particular, are involved in ATP-dependent proteolysis; examples include bacterial proteins ClpA, ClpB, ClpX, FtsH, and HslU; proteasome components; and yeast HSP78 (*7*). Members of the novel archaeal protein family could also perform chaperone-like functions. This is particularly plausible, because *M. jannaschii* does not encode several molecular chaperones that are ubiquitous and highly conserved in bacteria and eukaryotes—namely, members of the HSP70, HSP90, and HSP40 families. It remains to be seen how typical is this situation in archaea.

Finally, the family of putative ATPases contains a third strikingly conserved motif with two invariant histidines and one invariant cysteine (Fig. 1). Even though this motif did not show statistically significant similarity to any proteins in the database, this may be a specific metal-binding site, and some resemblance of the divalent cation-binding motif in bacterial Fur proteins that are metal-dependent transcription regulators (*8*) could be detected (Fig. 1). Two observations seem relevant: (i) One of the chaperone ATPases, FtsH, contains a metal-binding motif conserved in its bacterial and eukaryotic homologs and is a Zn-dependent protease (*9*). (ii) *Methanococcus jannaschii* encodes at least two other putative ATPases, namely, the predicted proteins MJ0578 and MJ0579 that also contain a metal-binding domain, in these cases a ferredoxin-like domain (*10*).

Thus, analysis of conserved motifs and application of additional methods for sequence database search yields specific functional predictions for archaeal proteins that initially appeared to comprise a unique family. There is little doubt that further exploration of the *M. jannaschii* genome sequence will bring more interesting findings.

Eugene V. Koonin, *National Center for Biotechnology Information, National Library of Medicine, National Institutes of Health, Bethesda, MD 20894, USA*

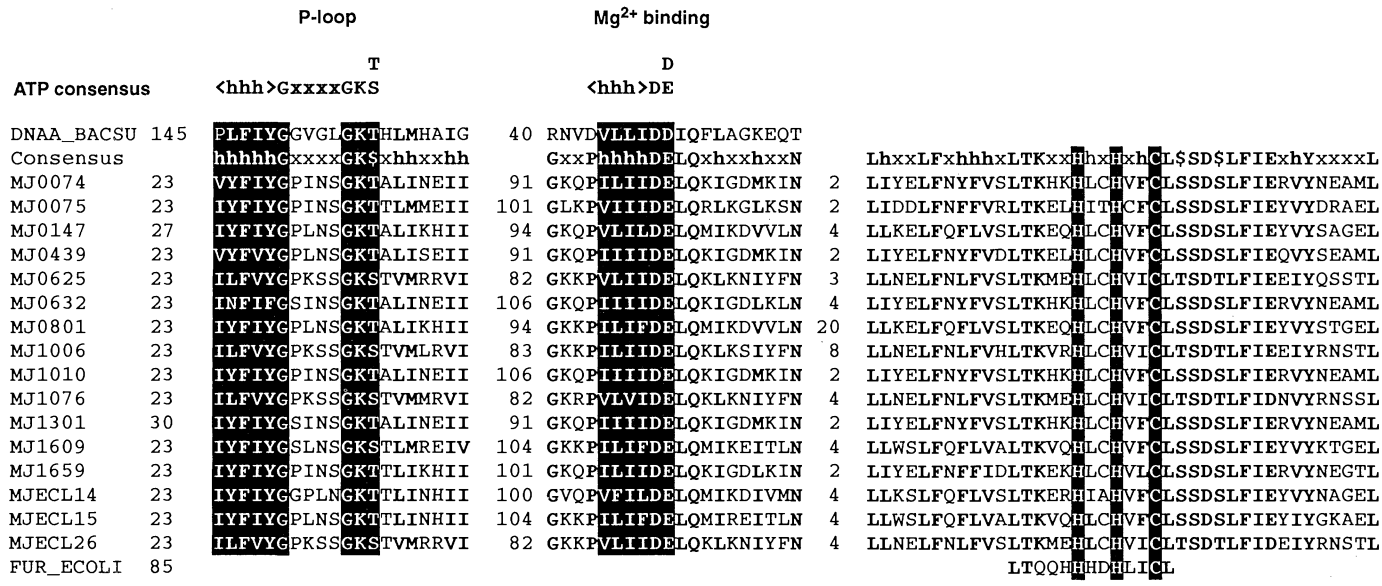

Fig 1. Alignment of the three conserved motifs in the novel family of putative archaeal ATPases. Alignment was constructed using the MACAW program (*11*). Consensus shows amino acid residues conserved in all of the 16 aligned sequences; h indicates a bulky hydrophobic residue (I, L, V, M, F, Y, W); $ indicates serine or threonine. Distances from the protein N-termini and distances between the alignment blocks are indicated by numbers. Fragments of the *Bacillus subtilis* DnaA protein and *Escherichia coli* Fur protein are shown for comparison. Two ATPase motifs and the conserved histidine and cysteine residues in the predicted metal-binding site are shown by reversed type. ATPase motif consensus is from (*4*); <hhh> indicates that three out of five residues preceding the first invariant G in the P-loop and the first D in the Mg^{2+}-binding motif are bulky and hydrophobic. In addition to the proteins shown, open reading frames MJ0819, MJ0820, and MJ0821 appear to represent remnants of a disrupted gene coding for a putative ATPase of the same family.

REFERENCES

1. C. J. Bult *et al.*, *Science* **273**, 1058 (1996).
2. J. E. Walker *et al.*, *EMBO J.* **1**, 945 (1982).
3. M. Saraste *et al.*, *Trends Biochem. Sci.* **15**, 430 (1990).
4. E. V. Koonin, *Nucleic Acids Res.* **21**, 2541 (1993).
5. S. F. Altschul *et al.*, *J. Mol. Biol.* **215**, 403 (1990).
6. S. F. Altschul and W. Gish, *Methods Enzymol.* **266**, 460 (1996).
7. F. Confalonieri and M. Duguet, *Bioessays* **17**, 639 (1995).
8. M. S. Lam *et al.*, *J. Bacteriol.* **176**, 5108 (1994).
9. T. Tomoyasu *et al.*, *EMBO J.* **14**, 2551 (1995).
10. A. R. Mushegian and E. V. Koonin, unpublished observations.
11. G. D. Schuler *et al.*, *Proteins Struct. Funct. Genet.* **9**, 180 (1991).

12 September 1996; accepted 16 January 1997

Aquaporins and Ion Conductance

A. J. Yool *et al.* studied membrane conductance in *Xenopus laevis* oocytes injected with aquaporin1 complementary RNA (*AQP1* cRNA) and concluded that the conductance observed represented an intrinsic property of the protein (*1*). We have reevaluated our own studies of the AQP1 protein and have conducted new experiments; our results support our earlier conclusion that AQP1 transports water, but does not conduct ions (*2*).

As measured in our laboratory (*2*), oocytes injected with water (as a control) or with *AQP1* cRNA exhibited similar, low conductances, while their permeabilities to water differed greatly [coefficient of osmotic water permeability (P_f)~10 μm/s and ~200 μm/s, respectively]. Because we had not previously investigated effects of forskolin on membrane-conductance, we used a two-electrode voltage clamp. Yool *et al.* (*1*) describe a rising scale of currents (measured in 100 mM NaCl, 2 mM KCl, 4.3 mM $MgCl_2$, and 5 mM Hepes; pH 7.3): water-injected oocytes rose 2.9 μA/V; AQP1 oocytes, 8.6 μA/V; and AQP1 oocytes with forskolin, 63 μA/V. In contrast, using standard conditions (frog Ringers solution: 115 mM NaCl, 2 mM KCl, 1 mM $CaCl_2$, 1 mM $MgCl_2$, and 5 mM Hepes; pH 7.4), we did not see any significant difference in membrane conductance when water-injected oocytes (n = 7) or AQP1 oocytes (n = 20) were compared before or after forskolin treatment (<1 μA/V for all measurements). We obtained similar results when $CaCl_2$ was omitted or when 0.5 mM 4.4′-diisothiocyanato-stilbene-2,2′-disulfonate (DIDS, Sigma, St. Louis, MO) was added to the solutions. Because AQP1 does not contain a classic cyclic AMP (cAMP)–dependent protein kinase A (PKA) phosphorylation consensus site, we performed experiments to evaluate oocytes that express AQP5 (which contains a classic PKA motif), but found that forskolin treatment also did not increase membrane currents of AQP5 oocytes (<1 μA/V in all measurements, n = 16).

The differences in membrane behaviors observed in our laboratories are not a result of the *AQP1* cDNA, because the construct used by Yool *et al.* came from our laboratory. Recently, we provided oocytes injected with *AQP1* cRNA in our laboratory to Yool *et al.*; when they analyzed these oocytes in their laboratory using their technique, forskolin-induced ion currents were observed (*3*). The explanation for this discrepancy is not known.

Peter Agre, M. Douglas Lee, Sreenivas Devidas, William B. Guggino, *Johns Hopkins University School of Medicine, Baltimore, MD 21205–2185, USA*

REFERENCES

1. A. J. Yool *et al.*, *Science* **273**, 1216 (1996).
2. G. M. Preston *et al.*, *ibid.* **256**, 385 (1992).
3. J. W. Regan, personal communication.

26 September 1996; accepted 27 January 1997

The description by Yool *et al.* (*1*) of the stimulation of cation permeability in AQP1